[CANCER RESEARCH 63, 7753–7759, November 15, 2003]

Reduced Hepatocyte Proliferation is the Basis of Retarded Liver Tumor Progression and Liver Regeneration in Mice Lacking *N*-Acetylglucosaminyltransferase III

Xiaoping Yang,[1] Jian Tang,[1] Charles E. Rogler,[2] and Pamela Stanley[1]

Departments of [1]Cell Biology and [2]Medicine, Albert Einstein College of Medicine, New York, New York

ABSTRACT

Mice lacking *N*-acetylglucosaminyltransferase III (GlcNAc-TIII) exhibit slightly but significantly retarded liver tumor progression after a single injection of 10 μg/g diethylnitrosamine (DEN) and continued administration of phenobarbital (PB) in drinking water. A key question is whether the absence of GlcNAc-TIII inhibits cell proliferation or induces apoptosis. Because PB aids tumor progression, we tested whether it diminished the difference in tumor progression between *Mgat3*$^{+/+}$ and *Mgat3*$^{\Delta/\Delta}$ mice. Here, we show that in the absence of PB, control males developed about twice as many liver tumor nodules as males lacking GlcNAc-TIII. Both the size of liver tumors and liver weights were significantly greater in DEN-treated wild-type or heterozygous mice. Apoptosis assays performed monthly after DEN treatment showed no differences between mutant and wild-type. However, there was a marked retardation in liver regeneration after partial (70%) hepatectomy (PH). Wild-type mice incorporated bromodeoxyuridine in ~15% of hepatocyte nuclei at 48 h after PH, whereas mice lacking GlcNAc-TIII had only ~5% positive nuclei. This was not because of enhanced apoptosis in mutant mice after PH. Expression of the *Mgat3* gene remained undetectable in wild-type liver by Northern analysis after tumor induction or after PH. In addition, transgenic overexpression of GlcNAc-TIII in hepatocytes did not enhance tumor progression in *Mgat3*$^{\Delta/\Delta}$ mice, and there were no differences in tumor progression or liver regeneration after PH between control and transgenic mice overexpressing GlcNAc-TIII in liver. Therefore, the nonhepatic action of GlcNAc-TIII promotes hepatocyte proliferation after PH, as well as the progression of DEN-induced tumors, providing evidence for a functional role of the bisecting GlcNAc on circulating glycoprotein growth factor(s) that stimulate hepatocyte proliferation.

INTRODUCTION

Evidence is accumulating of functions in tumor progression for individual sugar residues in complex glycans on cell surface glycoproteins. We have previously shown in mice lacking GlcNAc-TIII[3] that the bisecting GlcNAc of complex *N*-glycans (Fig. 1) is required for optimal tumor progression after induction of hepatocarcinogenesis by a single injection of DEN and treatment with PB (1, 2). Elimination of GlcNAc-TV and the branching β 1,6-linked GlcNAc of complex *N*-glycans (Fig. 1) in the mouse leads to retarded progression and reduced metastasis of mammary tumors (3). Mutant mice lacking P-selectin whose glycan ligand requires α1,3-fucose in the sialylated Lewis X determinant (Fig. 1) of a core 2 *O*-glycan (4) exhibit reduced tumor growth and metastasis in a lung cancer model (5). Tumor cells induced to express intermediate levels of sialylated Lewis X on surface glycoconjugates exhibit increased levels of lung colonization in a tail vein metastasis assay (6, 7). In addition to these functional studies, there are many correlations between the expression of specific glycans on cellular glycoconjugates and the progression of cancer cells to malignancy and metastasis in humans (8). However, molecular bases for the roles of sugars in tumor progression are not well understood.

To address mechanisms by which an individual sugar on complex *N*-glycans may influence tumor progression, we investigated whether the retarded tumor progression in mice lacking GlcNAc-TIII (1, 2) was reflected in retarded recovery from 70% PH and whether it was attributable to enhanced apoptosis in *Mgat3*$^{\Delta/\Delta}$ mice. We also investigated whether prolonged treatment with PB, a tumor promoter, diminished the difference in DEN-induced tumor progression between control and *Mgat3*$^{\Delta/\Delta}$ mice. The data show a greater reduction in tumor progression in *Mgat3*$^{\Delta/\Delta}$ mice than observed previously when PB was used after DEN (2). In addition, a markedly slower recovery from PH occurred in *Mgat3*$^{\Delta/\Delta}$ mice compared with wild-type controls. In neither case was the retarded response of *Mgat3*$^{\Delta/\Delta}$ mice attributable to increased apoptosis, and there was no effect on either response of expressing large amounts of GlcNAc-TIII in hepatocytes. The data provide evidence that the bisecting GlcNAc on the *N*-glycans of circulating glycoprotein(s) promotes hepatocyte proliferation during liver regeneration and tumor progression.

MATERIALS AND METHODS

Mouse Strains. *Mgat3*$^{\Delta/\Delta}$ mice carrying a deletion of the *Mgat3* gene coding region were generated from strain *Mgat3*^{tm1Jxm} mice (9) as described previously (2). Originally from a 129^{SvJ}/CD1 mixed background, this strain was maintained by brother:sister and cousin mating, and littermates were used in these experiments after more than six generations of inbreeding. *Mgat3*-transgenic mice expressing functional GlcNAc-TIII in liver under the control of the major urinary protein promoter, with six to seven copies of the *Mgat3* transgene at one integration site, were described previously (2). They were generated on a CBA/C57Bl/6 hybrid background and maintained by brother:sister and cousin matings. Crosses between *Mgat3*$^{\Delta/+}$ mutants and *Mgat3*-transgenic mice generated *Mgat3*$^{+/+}$, *Mgat3*$^{\Delta/+}$, and *Mgat3*$^{\Delta/\Delta}$ littermates carrying the *Mgat3* transgene. Mice were housed under pathogen-free conditions with food and water *ad libitum*. Experimental protocols were approved by the Animal Institute Committee at the Albert Einstein College of Medicine.

Hepatoma Induction and Analysis. Male pups received i.p. injections with DEN (Sigma) to induce liver cancer at 10–12 days after birth as in previous experiments (1, 2). Mice treated with PB were given 500 parts/million in drinking water 1 month after birth continuously until dissection. At various times after DEN injection, mice were dissected and livers excised to determine visible tumor numbers, the diameter of each tumor, the ratio of liver:kidneys and liver:body weights, and histopathological changes. Liver sections stained with H&E were scored in random order and blindly for the stage of hepatocarcinogenesis according to the numerical criteria previously described (2): 0, normal liver; 1, mild, localized dysplasia with mild disruption of hepatic cords and no discernible AHF; 2, moderate dysplasia with disruption of hepatic cords, AHF occupy <5% of the liver, and AHFs are ~1 mm in diameter; 3, severe dysplasia and disruption of cord structure, predominant AHF prevalent throughout the liver (encompass ≥20% of liver), and many exceed 2 mm

Received 5/14/03; revised 9/5/03; accepted 9/11/03.

Grant support: This work was supported by Albert Einstein Liver Center Pilot Project Grant NIH DK 41296, NIH Grant NCI RO1 30645 (to P. S.), and by partial support from the Albert Einstein Cancer Center Grant NCI PO1 13330.

Present address: Xiaoping Yang, Department of Cancer Biology, University of Pennsylvania School of Medicine, Philadelphia, PA 19104.

Present address: Jian Tang, Department of Medicine and Center for Study of the Tumor Microenvironment, Beth Israel Deaconness Medical Center and Harvard Medical School, Boston, MA 02215.

The costs of publication of this article were defrayed in part by the payment of page charges. This article must therefore be hereby marked *advertisement* in accordance with 18 U.S.C. Section 1734 solely to indicate this fact.

Requests for reprints: Pamela Stanley, Department of Cell Biology, Albert Einstein College of Medicine, 1300 Morris Park Avenue, New York, NY 10461. Phone: (718) 430-3346; Fax: (718) 430-8574; E-mail: stanley@aecom.yu.edu.

[3] The abbreviations used are: GlcNAc-T, *N*-acetylglucosaminyltransferase; DEN, diethylnitrosamine; PH, partial hepatectomy; PB, phenobarbital; BrdUrd, bromodeoxyuridine; ALT, alanine aminotransferase; AHF, altered hepatic foci; AST, aspartate aminotransferase; SDH, sorbital dehydrogenase; HCC, hepatocellular carcinoma; VEGF, vascular endothelial growth factor; EGF, epidermal growth factor.

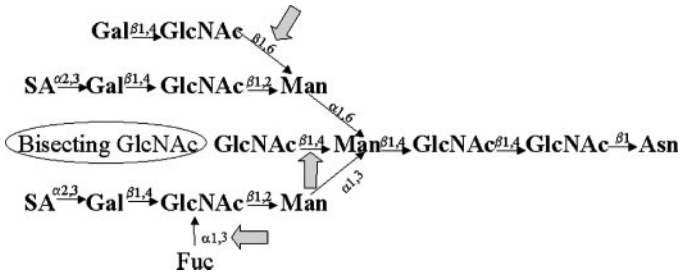

Fig. 1. Complex *N*-glycan with the bisecting GlcNAc. The *Mgat3* gene encodes GlcNAc-TIII, which generates *N*-glycans with a bisecting GlcNAc. GlcNAc-TV adds the β 1,6GlcNAc branch and various α 1,3 fucosyltransferases add the fucose that generates the sialylated Lewis X determinant recognized by selectins. Mice or tumor cells lacking the particular glycosyltransferase that catalyzes each of the linkages indicated by an *arrow* have reduced tumorigenesis (see text).

and appear as distinct nodules on the liver; 4, multiple, large neoplastic nodules present, some of which appear to be early tumors, classified as adenomas when they exceed ~4–5 mm; 5, clear HCC present, plus many earlier lesions, HCCs are few in number and rather small, with a predominantly differentiated phenotype; 6, many large HCCs present and some of the tumors have a poorly differentiated phenotype, although differentiated phenotypes are also present.

Seventy Percent PH. Seventy percent PH was performed on *Mgat3*$^{\Delta/\Delta}$ mice, *Mgat3*-transgenic mice, and their respective wild-type littermate controls. Male mice ages ~2 months were weighed and injected i.p. with 2.5% avertin (tribromomethylalcohol and tertiaryamylalcohol; Sigma) at 13–17 μl/g body weight. A 1-cm incision under the xiphoidprocess of the sternum was performed, and the left lateral and median lobes of the liver were squeezed out, ligated at the base with nonabsorbable suture thread, resected, weighed, and snap frozen in liquid nitrogen. The abdominal incision was sewn up with a first layer of peritoneum and abdominal muscles and a second layer of skin in an interrupted suture pattern. During surgery and recovery, a heat lamp was used to maintain the temperature of the mouse until it was fully conscious. Thereafter, mice were transported to a quarantine room and monitored daily. At different times after 70% PH, mice were bled from the retro-orbital sinus, and sera were stored at −80°C. i.p. injection of BrdUrd (Sigma) at 50 μg/g body weight was performed and 2 h later, mice were anesthetized, and remnant livers were resected and weighed. Pieces of liver were subsequently fixed in 10% buffered formalin (Fisher) while the remainder was snap frozen and stored at −80°C. Fixed liver pieces were paraffin embedded, sectioned, and analyzed in various ways.

Analysis of BrdUrd Incorporation. After drying at 55°C for 45 min, fixed liver sections from mice treated with BrdUrd were deparaffinized in Histoclear (National Diagnostics), rehydrated in a series of graded ethanols, and treated by the protocol recommended in the BrdUrd staining kit from Oncogene Research Products. Briefly, after quenching, denaturing, and blocking, slides were incubated at 37°C with biotinylated mouse anti-BrdUrd for 60 min, followed by Streptavidin-peroxidase for 10 min and 3,3′-diaminobenzidine for 6 min. Slides were counterstained with hematoxylin for 3 min before dehydration in a series of graded ethanols. After washing in Histoclear, stained slides were mounted with Histomount under coverslips. BrdUrd-positive and -negative nuclei of hepatocytes were counted in 10 randomly selected fields under ×400 magnification. BrdUrd incorporation was calculated as the percentage of BrdUrd-positive hepatocyte nuclei in the 10 fields.

TUNEL Assay for Apoptosis. TUNEL assays for DNA fragmentation were performed with a TUNEL assay kit (Intergen Company) according to the manufacturer's instructions to evaluate apoptosis in livers with hepatoma or at various times after PH. Liver sections were deparaffinized in Histo-clear and rehydrated in ethanols (95% and 70%) before treatment with proteinase K (Sigma, 20 μg/ml) for 20 min. After quenching and equilibration, terminal deoxynucleotidyltransferase was added to the slide, and after 1 h at 37°C, the reaction was terminated. After washing in PBS, antidigoxigenin peroxidase conjugate was incubated on the slide for 30 min 37°C before the addition of 3,3′-diaminobenzidine substrate for 4 min. Slides were counterstained with 0.1% methyl green for 10 min, washed with 1-butanol and Histo-clear, and finally mounted with coverslips over Histomount. TUNEL-positive and -negative hepatocyte nuclei were counted in 20 randomly chosen fields at a magnification of ×400 by light microscopy.

Liver Function Tests. Serum samples that had been stored at −80°C since collection on the day of liver harvest were thawed on ice, mixed completely, and aliquots of 70 μl were refrozen. They were subsequently sent to Ani Lytics Incorporated (Gaithersburg, MD) where a standard automated clinical analyzer was used to assay ALT, AST, SDH, total protein, and total bilirubin.

RNA Isolation and Northern Analysis. TRIzol reagent (Life Technologies, Inc.) was used to isolate total RNA from frozen livers or kidneys, according to protocols provided by the manufacturer. An oligo(dT) column (Pharmacia) was used to purify poly(A)$^+$ RNA from total RNA. Poly(A)$^+$ RNA (10 μg) was electrophoresed on a 1.2% denaturing agarose gel and transferred to a nylon membrane (Amersham). After cross-linking, the membrane was prehybridized and hybridized overnight at 60°C, respectively, in buffer containing 50 mM piperazine-*N*, *N*′-bis(2-ethanesulfonic acid) (pH 6.5), 0.1 M NaCl, 50 mM sodium phosphate buffer, 0.5 mM EDTA, 5% SDS, and 60 μg/ml herring sperm DNA. The membrane was probed with a DNA probe labeled with ^{32}P-dCTP (6000 Ci/mmol; New England Nuclear) using the Prime-it radioactive labeling kit (Stratagene). The membrane was washed in 2× SSC and 0.1% SDS solution for 20 min at room temperature and subsequently for 30 min at 60°C before being exposed to Kodak X-OMAT films at −80°C with or without intensifying screens.

Serum VEGF Assay. Serum VEGF levels were determined after the procedures of the mouse VEGF immunoassay kit (R&D Systems). Sera diluted 5-fold in buffer provided in the kit (50 μl) were incubated for 2 h at room temperature in 96-well plates coated with mouse VEGF antibody and then incubated with the ant-mouse VEGF conjugate for an additional 2 h. After incubation with hydrogen peroxide and tetramethylbenzidine for 30 min at room temperature, reactions were stopped, and the *A* at 450 nm was determined using an ELISA reader. A standard curve was generated with standards provided, and VEGF concentrations were calculated using Excel software.

Statistical Analyses. Mean, SD, SE, student *t* test, linear regression and correlation, and other calculations were performed using either Excel software or InStat 2.01 software.

RESULTS

Enhanced Role for GlcNAc-TIII in DEN-Induced Hepatocarcinogenesis in the Absence of PB. We previously showed that after DEN induction and long-term PB treatment, hepatoma progression is retarded in two different mutant strains of mice lacking GlcNAc-TIII because of targeted inactivation of the *Mgat3* gene [*Mgat3*$^{neo/neo}$ (1, 2) now termed *Mgat3*$^{T37/T37}$ (10) and *Mgat3*$^{\Delta/\Delta}$ (2)]. However, the reduction in hepatoma formation is significantly less in *Mgat3*$^{\Delta/\Delta}$ mice compared with *Mgat3*$^{T37/T37}$ mice (2), perhaps because the latter express truncated, inactive GlcNAc-TIII (10). Conditions were therefore sought to enhance the differential in hepatoma progression between *Mgat3*$^{\Delta/\Delta}$ and *Mgat3*$^{+/+}$ mice. Because PB is a promoter of tumor progression (11) and might diminish differences in rates of progression, a DEN only dose response study was performed. *Mgat3*$^{+/+}$, *Mgat3*$^{+/\Delta}$, and *Mgat3*$^{\Delta/\Delta}$ male mice were injected at 12 days after birth with 10, 25, 50, or 100 μg DEN/g body weight. The highest dose was very toxic and was not pursued. At 6 months after injection, control mice of each genotype had no tumors, whereas *Mgat3*$^{+/+}$ and *Mgat3*$^{\Delta/+}$ mice had similar numbers of tumors [112 ± 23 at 10 μg/g (n = 10) and 127 ± 9 at 50 μg/g (n = 14)]. Importantly, homozygous *Mgat3*$^{\Delta/\Delta}$ mice had ~50% fewer tumors [66 ± 28 at 10 μg/g (n = 3) and 60 ± 8 at 50 μg/g (n = 4)]. Thus in the absence of PB, the loss of GlcNAc-TIII had a much greater effect on slowing tumor progression in *Mgat3*$^{\Delta/\Delta}$ mice.

To begin to address mechanism, mice were treated with DEN at 50 μg/g body weight and analyzed from 2 through 6 months after DEN injection for tumor formation and apoptosis. At 2 months after DEN injection, no tumors were visible, at 3 months mice in the treated group displayed 2 to 4 tiny tumors/liver, and at 4 months, a variable number of small tumors was present in the treated groups. A significant difference in tumor numbers between *Mgat3*$^{+/+}$ or *Mgat3*$^{+/\Delta}$ and *Mgat3*$^{\Delta/\Delta}$ mice occurred at 5 and 6 months after DEN treatment

(Fig. 2). There was no significant gene dosage effect as *Mgat3*$^{+/+}$ and heterozygote *Mgat3*$^{+/\Delta}$ mice had similar tumor numbers. Tumor sizes were compared between *Mgat3*$^{+/+}$ and *Mgat3*$^{\Delta/\Delta}$ mice by measuring the diameter of each nodule and the numbers in each of five categories were averaged (Table 1). At 3 and 4 months, tumors were small and no significant difference was found between *Mgat3*$^{+/+}$ and *Mgat3*$^{\Delta/\Delta}$ mice. However, at 5 and 6 months after DEN, *Mgat3*$^{\Delta/\Delta}$ mice had only about half the number of tumors of *Mgat3*$^{+/+}$ mice in the groups of 1–3, 3–5, 5–7, and >7 mm, whereas they had equivalent numbers of tiny tumors (0–1 mm category). Clearly, *Mgat3*$^{\Delta/\Delta}$ mice displayed fewer and smaller tumor foci on the liver surface than control mice. In addition, liver mass reflected tumor burden. In control mice, no significant change in the ratios of liver:kidneys or liver:body weights were observed between *Mgat3*$^{+/+}$ and $^{+/\Delta}$ and *Mgat3*$^{\Delta/\Delta}$. In contrast, after DEN treatment, liver weight increased in control and mutant groups at 5 and 6 months. At 6 months, the weight ratio for *Mgat3*$^{+/+}$ and $^{+/\Delta}$ mice was 6.7 ± 0.3 and for *Mgat3*$^{\Delta/\Delta}$ mice it was 5 ± 0.7, a significant difference ($P = 0.03$). Thus at 5 and 6 months after DEN, *Mgat3*$^{\Delta/\Delta}$ mice displayed fewer tumors of smaller diameter and a reduced tumor burden compared with wild-type littermates.

Histological analysis of liver sections taken at each month after DEN was performed to monitor tumor progression (Fig. 3). Slides were scored at random and blindly according to numerical criteria scaled 0 through 6 (Ref. 2, see "Materials and Methods"), with 0 representing normal liver and 6 representing severe, poorly differentiated HCC. At 2 months, most DEN-treated livers displayed intact liver architecture and few exhibited mild disruption of hepatic cords, consistent with the lack of obvious tumors at that time point. At 3 months, AHF were found in each group of mice with wide histological changes from normal liver to HCC, but in general, no apparent difference in hepatocarcinogenesis was found between *Mga3*$^{+/+}$ and *Mgat3*$^{\Delta/\Delta}$ mice. Significant differences in pathohistological changes between wild-type and mutant mice occurred at 4, 5, and 6 months. At 4 months, the majority of wild-type mice had developed some HCC that were small and of a predominantly differentiated type and many adenomas (score 5), whereas *Mgat3*$^{\Delta/\Delta}$ mice showed enormous histological variation from mild AHF (score 2), to adenoma (score 4), to HCC in a few mice (score 5). The most severe histological change of HCC with a poorly differentiated phenotype (score 6) was achieved in all *Mgat3*$^{+/+}$ mice at 5 and 6 months, whereas *Mgat3*$^{\Delta/\Delta}$ liver sections mostly scored 4 or 5 and only rarely reached a score of 6 at those same time points.

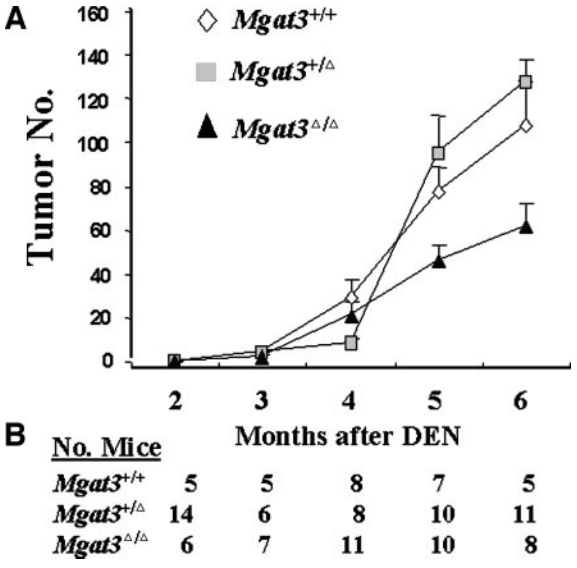

Fig. 2. Tumor numbers in *Mgat3*$^{+/+}$, *Mgat3*$^{+/\Delta}$, and *Mgat3*$^{\Delta/\Delta}$ mice treated with DEN. *A*, male littermates of 12 days were injected with a single dose of DEN at 50 μg/g body weight and numbers of visible tumor nodules on the liver surface were counted. *Error bars* are SE. Significance determined from two-tailed Student *t* test. *B*, number of mice at each time point.

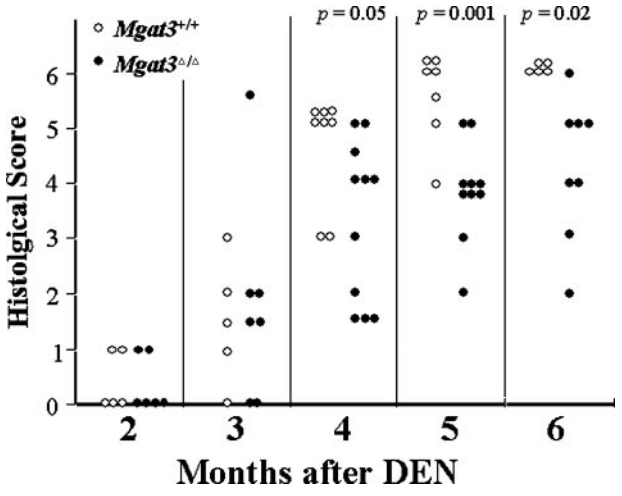

Fig. 3. Histological scores of hepatocarcinogenesis in *Mgat3*$^{+/+}$ and *Mgat3*$^{\Delta/\Delta}$ mice. Liver sections (~4–8/mouse) of 5-μm thickness fixed in 10% formalin and H&E stained were scored at random and blindly, according to a numerical criteria scaled from 0 (normal liver) through 6 (poorly differentiated HCC) as described in "Materials and Methods" and "Results." Each circle represents an individual mouse. The scores from different sections for each mouse were averaged and plotted. Significance was determined by the two-tailed Student *t* test.

The retarded hepatoma progression in *Mgat3*$^{\Delta/\Delta}$ mice could be attributable to decreased proliferation of transformed cells or enhanced apoptosis of hepatocytes in *Mgat3*$^{\Delta/\Delta}$ mice. Apoptosis was examined using the TUNEL assay in liver sections from *Mgat3*$^{+/+}$ and *Mgat3*$^{\Delta/\Delta}$ mice at 2–5 months after DEN treatment. Apoptotic hepatocytes were <3/20 fields counted at ×400 magnification in *Mgat3*$^{+/+}$ and *Mgat3*$^{\Delta/\Delta}$ mice treated with DEN. The total number of apoptotic cells increased to 7–15/20 fields counted in two to four sections/mouse at 2 and 3 months after DEN treatment and subse-

Table 1 *Distribution of tumor sizes in Mgat3*$^{+/+ \text{ and } +/\Delta}$ *and Mgat3*$^{\Delta/\Delta}$ *liver after DEN treatment*

Time after DEN (mo)	Genotype (no. mice)	No. tumors in each category				
		0–1 mm[a] Average ± SE	1–3 mm Average ± SE	3–5 mm Average ± SE	5–7 mm Average ± SE	>7 mm Average ± SE
3	*Mgat3*$^{+/+ \text{ and } +/\Delta}$ (11)	3 ± 1	1 ± 0			
3	*Mgat3*$^{\Delta/\Delta}$ (7)	1 ± 1	1 ± 0			
4	*Mgat3*$^{+/+ \text{ and } +/\Delta}$ (16)	12 ± 4	7 ± 2			
4	*Mgat3*$^{\Delta/\Delta}$ (11)	12 ± 3	10 ± 3			
5	*Mgat3*$^{+/+ \text{ and } +/\Delta}$ (15)	21 ± 2	45 ± 6	7 ± 2	2 ± 0	1 ± 1
5	*Mgat3*$^{\Delta/\Delta}$ (10)	17 ± 4	26 ± 5	2 ± 1	0 ± 0	1 ± 0
6	*Mgat3*$^{+/+ \text{ and } +/\Delta}$ (6)	25 ± 3	64 ± 12	16 ± 4	5 ± 2	3 ± 2
6	*Mgat3*$^{\Delta/\Delta}$ (8)	20 ± 5	32 ± 5	6 ± 3	2 ± 1	1 ± 1

[a] The diameter of each tumor on the liver surface was measured with calipers and averaged.

quently decreased to 4–6/20 fields at 5 months after DEN. However, the majority of these were endothelial cells based on their location and morphology. In addition, there was no significant difference between wild-type and mutant mice in their apoptotic index after DEN treatment.

Retarded Liver Regeneration After PH in *Mgat3*$^{\Delta/\Delta}$ Mice. To investigate a potential effect of the lack of GlcNAc-TIII on hepatocyte proliferation, wild-type and mutant mice were compared for liver regeneration after 70% PH. At 8–10 weeks of age, *Mgat3*$^{+/+}$ and *Mgat3*$^{\Delta/\Delta}$ male littermates were subjected to 70% PH. Two h before dissection, mice were orbitally bled and injected with 50 μg BrdUrd/g body weight to label newly synthesized DNA. At various times, post-PH blood was drawn, livers were harvested, weighed, sectioned, and stained with antibodies to BrdUrd. Resected liver portions were weighed to calculate the degree of liver regeneration. To monitor liver function in hepatecomized mice, total protein, bilirubin, ALT, AST and SDH were assayed in sera. A reduced level of serum protein often correlates with liver disease, bilirubin is used in the diagnosis of jaundice, and increased levels of ALT, AST, and SDH are indicators of liver damage because of hepatocyte cell death. ALT, AST, SDH, and bilirubin were dramatically increased at 24 h after PH and subsequently gradually decreased similarly in both *Mgat3*$^{+/+}$ and *Mgat3*$^{\Delta/\Delta}$ mice (supplementary Fig. 1). In contrast, total serum protein was reduced at 24 h after PH and increased gradually although not completely to normal levels by 96 h after PH. There was no significant difference in total protein, bilirubin, AST, ALT, and SDH between *Mgat3*$^{+/+}$ and *Mgat3*$^{\Delta/\Delta}$ mice during liver regeneration. There was also no difference in survival after PH which was ~80% for both wild-type and mutant mice. The only difference was found in SDH before surgery. *Mgat3*$^{\Delta/\Delta}$ mice had an increased level of SDH (31 compared with 8.2 units/liter in control; $P < 0.00001$).

To determine cell proliferation after PH, BrdUrd-positive and -negative hepatocytes were counted in liver sections, and the percentage of BrdUrd incorporation was calculated. BrdUrd incorporation was dramatically decreased in *Mgat3*$^{\Delta/\Delta}$ mice at 48 h (4.7 compared with 15% in control) and at 72 h (3.2 compared with 9.7% in control) after PH (Fig. 4). Therefore, PH-stimulated hepatocyte DNA synthesis was significantly inhibited in *Mgat3*$^{\Delta/\Delta}$ mice. This was reflected in a decrease in regenerated liver mass at 72 h (61 compared with 76% in control) and decreased remnant liver mass at 48 h (0.87 compared with 1.02 g in control). Therefore, liver regeneration was markedly impaired in *Mgat3*$^{\Delta/\Delta}$ mice based on BrdUrd incorporation into hepatocytes, percentage of regenerated liver mass, and remnant liver mass.

We also investigated apoptosis in regenerating livers from *Mgat3*$^{+/+}$ and *Mgat3*$^{\Delta/\Delta}$ mice. At 24, 36, 48, and 72 h after PH total apoptotic cells ranged from two to four cells/20 fields/two to four sections from each mouse at ×400 magnification, whereas apoptotic hepatocytes were extremely rare. No significant difference in apoptosis was found between hepatectomized *Mgat3*$^{+/+}$ and *Mgat3*$^{\Delta/\Delta}$ mice at any time point after PH. Therefore, the difference in hepatoma progression observed at 4–6 months (Fig. 2) and the difference in liver regeneration at 48 and 72 h (Fig. 4) are attributable to decreased hepatocyte proliferation rather than enhanced apoptosis in *Mgat3*$^{\Delta/\Delta}$ mice.

Serum VEGF Levels in Mice Treated with DEN and after 70% PH. VEGF is an endothelial cell-specific mitogen that functions in vasculogenesis and angiogenesis, and serum VEGF levels are correlated with hepatoma progression in humans (12). Thus, VEGF serum level is a good biological marker for prognosis of HCC. Interestingly, VEGF is a glycoprotein with *N*-glycans that carry the bisecting GlcNAc, and glycosylation is essential for its efficient secretion (13) but dispensable for its function (14). So it was important to measure the serum levels of VEGF in DEN-treated mice. Both *Mgat3*$^{+/+}$ and *Mgat3*$^{\Delta/\Delta}$ mice showed a linear correlation ($P < 0.05$) between serum VEGF levels and their stage of hepatocarcinogenesis (tumor number or liver weight or ratio of liver:kidneys weights). At 5 and 6 months, serum VEGF levels were increased compared with those at 4 months in wild-type mice but not in *Mgat3*$^{\Delta/\Delta}$ mice (Table 4). In addition, a significant difference in serum VEGF levels was observed between DEN-treated *Mgat3*$^{+/+}$ and *Mgat3*$^{\Delta/\Delta}$ mice at 5 and 6 months (Table 2).

During liver regeneration after PH, VEGF is increased in hepatocytes at 48–72 h after PH (15). Injection of VEGF promotes the proliferation of hepatocytes and endothelial cells at 48 h after PH, whereas neutralization of VEGF inhibits the proliferation of hepatocytes and endothelial cells (15). So VEGF is an important factor in promoting liver regeneration. However, at 48 h after PH when a highly significant reduction in BrdUrd incorporation was observed in *Mgat3*$^{\Delta/\Delta}$ mice (Fig. 4), both *Mgat3*$^{+/+}$ and *Mgat3*$^{\Delta/\Delta}$ mice had similar serum VEGF levels (59.51 and 63 pg/ml, respectively). Therefore, VEGF level does not appear to be responsible for the retarded liver regeneration observed in *Mgat3*$^{\Delta/\Delta}$ mice after PH.

Expression of the *Mgat3* Gene in Hepatocarcinogenesis and during Liver Regeneration. *Mgat3* gene expression and GlcNAc-TIII activity are induced in preneoplastic liver tissue and hepatomas of humans and rats (16–21). By contrast, we reported that *Mgat3* gene transcripts are not detectable by Northern analysis of mouse hepatoma tissues treated with DEN and PB for 7 months (1, 2). The same result was obtained in this study with livers from wild-type mice treated with DEN (but no PB) through 6 months. No significant induction of *Mgat3* gene expression was observed by Northern analysis (Fig. 5*A*). During liver regeneration in rat, both *Mgat3* gene transcripts and GlcNAc-TIII activity increase ~2-fold (17). However, *Mgat3* gene transcripts were not significantly induced in wild-type regenerating mouse liver after PH (Fig. 5*B*). This suggests as observed previously (2) that it is the lack of GlcNAc-TIII in a tissue other than liver that is responsible for retarded tumor progression and liver regeneration in *Mgat3*$^{\Delta/\Delta}$ mice. To test this hypothesis, the effects of DEN treatment in the absence of PB and PH were examined in mice overexpressing GlcNAc-TIII in liver.

Hepatocarcinogeneisis and Liver Regeneration in Mice Overexpressing the *Mgat3* Gene in Liver. To examine hepatocarcinogenesis in mice carrying a transgene with the *Mgat3* gene coding region expressed under the control of the major urinary protein promoter (2), transgenic males were treated with DEN at 50 μg/g body weight. At 5 months after DEN injection, *Mgat3* transgenic and nontransgenic littermates were dissected and analyzed. No significant difference was observed between control and transgenic mice treated with DEN, based on liver burden, tumor numbers, and histological examination (Table 3). An experiment performed under the previous regimen (single injection of 10 μg/g DEN followed at 1 month by continuous PB in water; Ref. 2) showed that the *Mgat3* transgene did not rescue tumor progression in *Mgat3*$^{\Delta/\Delta}$ mice (Table 4). *Mgat3*$^{+/+}$ mice overexpressing GlcNAc-TIII in liver had ~50 tumors after 7 months compared with ~30 in *Mgat3*$^{\Delta/\Delta}$ mice expressing the transgene. This experiment also shows that retarded tumor progression occurred in mice of different, mixed genetic background.

Liver regeneration was impaired in *Mgat3*$^{\Delta/\Delta}$ mice (Fig. 4), but *Mgat3* gene transcripts were not significantly induced in regenerating liver of *Mgat3*$^{+/+}$ mice (Fig. 5*B*). No effect on the rate of liver regeneration after PH was observed in mice overexpressing GlcNAc-TIII in liver (Fig. 6). *Mgat3*-transgenic mice displayed the same time course of BrdUrd incorporation and increase in regenerated liver mass

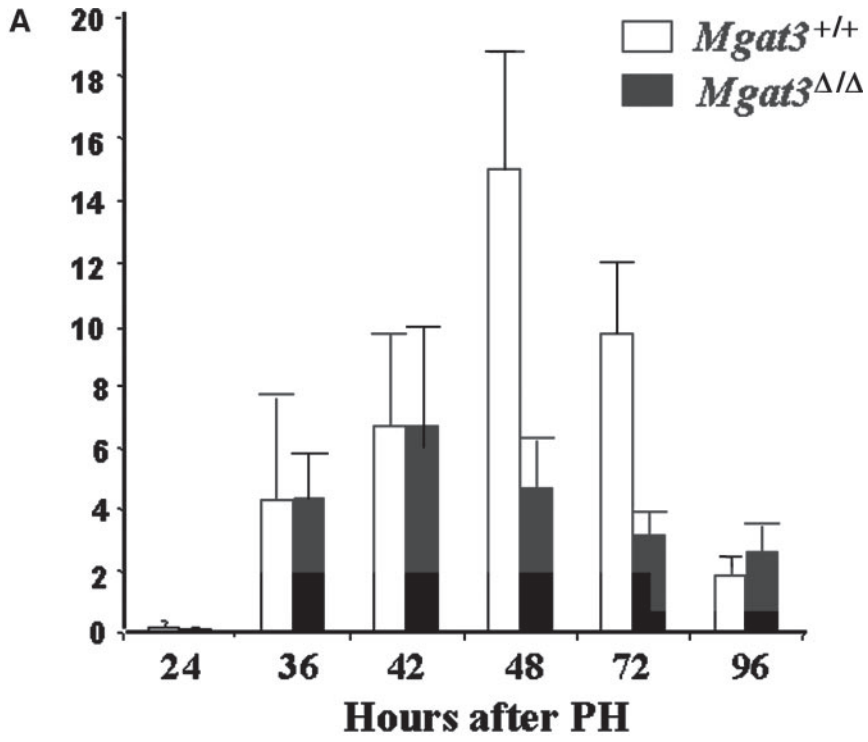

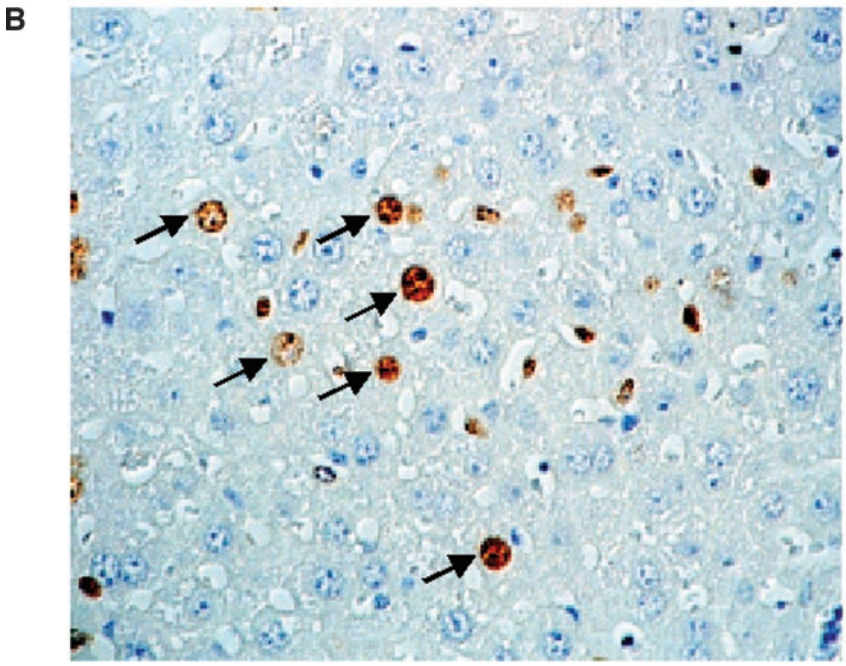

Fig. 4. BrdUrd incorporation in *Mgat3*$^{+/+}$ and *Mgat3*$^{\Delta/\Delta}$ mice after PH. After immunostaining fixed liver sections with BrdUrd antibody, BrdUrd-positive and -negative hepatocytes were counted in 10 fields at ×400 magnification. BrdUrd incorporation was determined by the percentage of BrdUrd-positive nuclei. *A*, BrdUrd incorporation at various time points after PH. Data are presented as average ± SE. n = at least 5/group. *B*, BrdUrd incorporated into regenerating liver at 48 h after pH in a wild-type mouse. Arrows point to hepatocytes that incorporated BrdUrd.

as control mice, suggesting that the course of liver regeneration was not altered at all in *Mgat3*-transgenic mice. Taken together, an extrahepatic role of the bisecting GlcNAc on circulating glycoprotein(s) is implicated in the mechanism of optimal liver regeneration.

Table 2 *Serum VEGF levels in Mgat3*$^{+/+}$ *and Mgat3*$^{\Delta/\Delta}$ *mice treated with DEN*
Data are average ± SE; n = number of mice.

Months after DEN	*Mgat3*$^{+/+}$ (pg/ml)	*n*	*P*	*Mgat3*$^{\Delta/\Delta}$ (pg/ml)	*n*	*P*
4	69.4 ± 8.2	8		71.1 ± 3.0	9	
5 and 6	115 ± 14.6	12	0.028[a]	87.8 ± 28.4	17	0.0385[b]

[a] Student t test.
[b] One-tailed t test.

DISCUSSION

We previously showed that mice lacking GlcNAc-TIII and therefore unable to add the bisecting GlcNAc to *N*-glycans on glycoproteins progress through DEN-induced hepatocarcinogenesis at a slower rate than wild-type mice (1, 2). We presented evidence that this difference is attributable to reduced tumor progression in *Mgat3*$^{\Delta/\Delta}$ mice. In this study, we provide insight into mechanism by showing that reduced hepatocyte proliferation rather than increased hepatocyte apoptosis is the basis of the retarded tumor progression as well as retarded liver regeneration after PH in *Mgat3*$^{\Delta/\Delta}$ mice.

We report here a marked enhancement of the difference in liver tumor progression between *Mgat3*$^{+/+}$ and *Mgat3*$^{\Delta/\Delta}$ mice in the

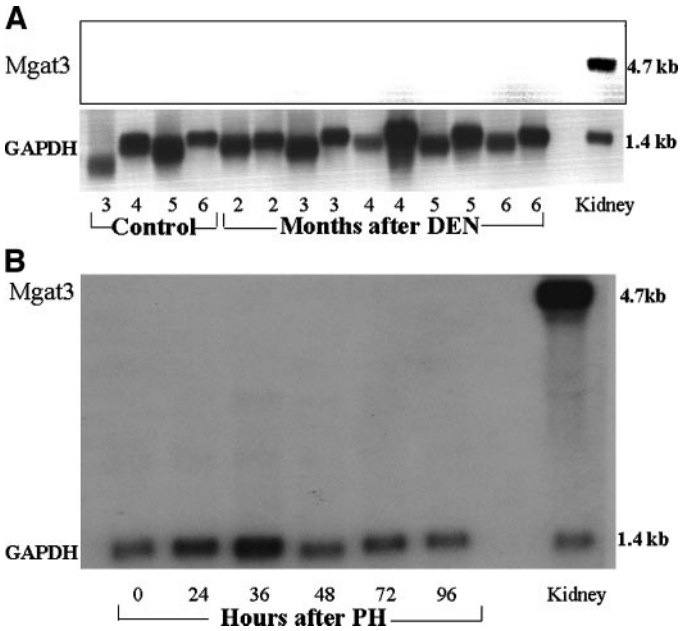

Fig. 5. *Mgat3* gene expression in liver cancer and liver regeneration. Poly A^+ RNA (10 μg) from liver and 20 μg total RNA from kidney of a wild-type mouse were subjected to Northern analysis and probed with a *Mgat3* gene coding region probe. After exposure to film, the membrane was stripped and rehybridized with a GAPDH probe. *A*, *Mgat3* gene expression in mouse liver cancers. RNA from livers of control and DEN wild-type mice of 2–6 m. *B*, *Mgat3* gene expression in regenerating livers from wild-type mice. RNA from regenerating livers at 0, 24, 36, 48, 72, and 96 h after 70% PH.

absence of PB treatment. PB is often used as a promoter to stimulate hepatoma progression, although it has complex effects [reviewed in Ref. (22)]. After injection of 50 μg/g DEN and no PB treatment, there was a ~2-fold reduction in tumor numbers visible on the liver surface of $Mgat3^{\Delta/\Delta}$ mice (Fig. 2, Table 1), whereas no significant difference in tumor number was obtained 7 months after injecting 10 μg/g DEN and administering PB (2). In the latter case, retarded tumor progression in $Mgat3^{\Delta/\Delta}$ mice was reflected in reduced liver weight. PB can affect the expression of at least 50 genes, and it can increase liver and kidney weights (23). After 7 months of PB administration, there was a significant increase in liver (~0.7 g) and in kidney (~0.14 g) weights in $Mgat3^{\Delta/\Delta}$ mice compared with PB-treated $Mgat3^{+/+}$ mice (2). This difference in response to PB could be one of the reasons for the small differential in tumor progression between $Mgat3^{+/+}$ and $Mgat3^{\Delta/\Delta}$ mice treated with DEN and PB (2) compared with DEN alone (this study).

Histological differences in hepatoma progression between $Mgat3^{+/+}$ and $Mgat3^{\Delta/\Delta}$ mice were not observed until 4 months (Fig. 3). This time course provides additional evidence that it is progression rather than initiation of hepatocarcinogenesis that is inhibited in $Mgat3^{\Delta/\Delta}$ mice, consistent with previous studies that showed that the number of AHF induced by DEN is similar in $Mgat3^{+/+}$- and *Mgat3*-knockout mice (1). TUNEL assays revealed no significant difference in apoptosis in liver sections of $Mgat3^{+/+}$ and $Mgat3^{\Delta/\Delta}$ mice treated with DEN at 2, 3, 4, or 5 months, so the retarded progression in $Mgat3^{\Delta/\Delta}$ mice appears to be attributable to inhibited hepatocyte proliferation, rather than enhanced apoptosis. Consistent with this is the finding that circulating VEGF levels in serum were not increased in DEN-treated $Mgat3^{\Delta/\Delta}$ mice (Table 2). VEGF levels in serum are positively correlated with hepatoma progression (12, 24), and VEGF synthesis is increased in proliferating hepatocytes (25). We observed increased serum VEGF levels in mice treated with DEN for 5 or 6 months compared with mice treated with DEN for 4 m. In addition, $Mgat3^{+/+}$ mice had substantially greater serum VEGF levels than $Mgat3^{\Delta/\Delta}$ mice. The decreased VEGF levels in $Mgat3^{\Delta/\Delta}$ mice at 5 and 6 months were not a direct effect of the absence of the bisecting GlcNAc because the same amount of VEGF was found in $Mgat3^{+/+}$ and $Mgat3^{\Delta/\Delta}$ sera at 4 months after DEN or at 48 h after PH when the greatest difference in BrdUrd incorporation was observed.

The motive for investigating liver regeneration in $Mgat3^{\Delta/\Delta}$ mice was to determine whether the retarded hepatoma progression of $Mgat3^{\Delta/\Delta}$ mice is reflected in liver regeneration, which would establish a rapid assay with which to investigate molecular mechanism. In fact, the results are most encouraging. $Mgat3^{\Delta/\Delta}$ mice were found to have decreased BrdUrd incorporation at 48 and 72 h after PH (Fig. 4) and decreased remnant liver weight or percentage of regenerated liver mass compared with controls. Therefore, liver regeneration after PH is impaired in $Mgat3^{\Delta/\Delta}$ mice, although liver function in $Mgat3^{\Delta/\Delta}$ and $Mgat3^{+/+}$ mice is similar (supplementary Fig. 1).

GlcNAc-TIII activity varies during the cell cycle of human colon cancer cells (26) and in a human hepatocarcinoma cell line (27), suggesting a potential autocrine effect of a glycoprotein growth factor or receptor that is enhanced by the presence of the bisecting GlcNAc. EGF is important in liver regeneration (28), and overexpression of the *Mgat3* gene may enhance EGF signaling depending on the cell line (29, 30). GlcNAc-TIII is up-regulated in human liver cancer (31, 32), rat liver tumors (2, 19), and regenerating rat liver (33). However, the mouse *Mgat3* gene is not induced in liver during hepatocarcinogenesis [(Ref. 1) and Fig. 5*A*), nor during liver regeneration (Fig. 5*B*). Most significantly, overexpression of an *Mgat3* gene in hepatocytes did not change the rate of liver regeneration (Fig. 6), nor the course of hepatocarcinogenesis (Table 3). The combined data reveal a noncell autonomous role for the bisecting GlcNAc in promoting hepatoma progression and liver regeneration in the mouse. Circulating glycoprotein growth factors such as EGF are predicted to be reduced in

Table 4 *Hepatoma progression in $Mgat3^{+/+}$, $Mgat3^{\Delta/+}$, and $Mgat3^{\Delta/\Delta}$ mice expressing the Mgat3 transgene in liver*

Transgenic mice expressing the *Mgat3* transgene in liver were crossed with $Mgat3^{\Delta/+}$ mice to generate $Mgat3^{+/+}$, $Mgat3^{\Delta/+}$, and $Mgat3^{\Delta/\Delta}$ mice expressing the transgene. Male littermates of each genotype were treated with DEN (10 μg/g body weight) and PB and analyzed at 7 months. Data are average ± SE.

	$Mgat3^{+/+}$	$Mgat3^{\Delta/+}$	$Mgat3^{\Delta/\Delta}$
Mgat3 transgene	+	+	+
No. mice	8	16	7
Tumor no.	51 ± 17	44 ± 11	32 ± 13
Liver:kidneys (wt)	7 ± 0.9	7.8 ± 1	5.4 ± 0.9
Liver:body (wt)	8.5 ± 1.3	9 ± 1.3	6.8 ± 1.3

Table 3 *Hepatoma progression in $Mgat3^{+/+}$ mice expressing the Mgat3 transgene in liver*

	Control	Control	P^a	DEN[b]	DEN[b]	P^a
Mgat3 transgene	−	+		−	+	
No. mice	13	11		13	16	
Tumor no.	0	0		50 ± 37	39 ± 25	0.37
Liver:kidneys (wt)	3.3 ± 0.4	3.4 ± 0.30	0.68	4.3 ± 1.54	4.00 ± 0.73	0.49
Liver:body (wt)	0.05 ± 0.01	0.04 ± 0.01	0.15	0.06 ± 0.02	0.06 ± 0.01	0.35
Histological score	0	0		4	4	

[a] Data are average ± SE; P = probability determined by student t test.
[b] DEN (50 μg/g body weight).

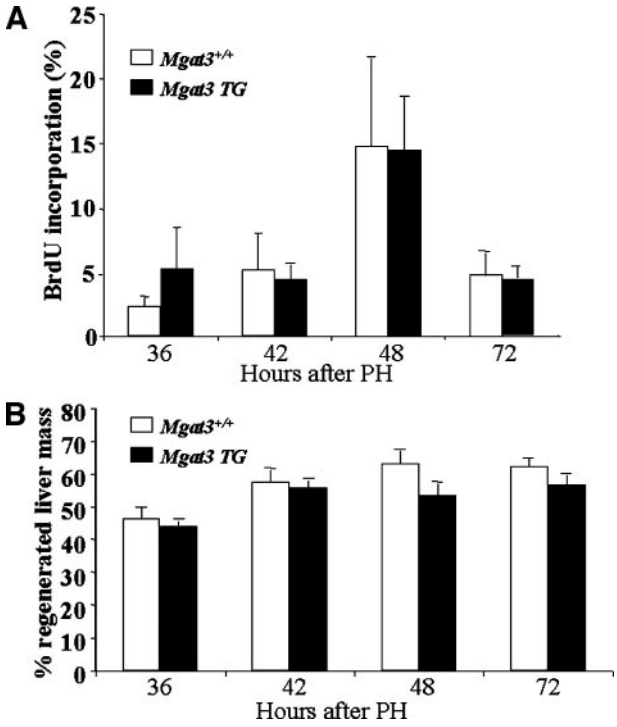

Fig. 6. Liver regeneration after PH in Mgat3-transgenic mice. Wild-type mice and Mgat3-transgenic mice were subjected to PH and regenerating livers were labeled with BrdUrd and harvested for analysis at 36, 42, 48, and 72 h after surgery. BrdUrd-positive and -negative hepatocytes were counted, and the percentage of positives is plotted. Data are presented as average ± SE. n = at least 5/group.

amount or growth factor activity in the serum of $Mgat3^{\Delta/\Delta}$ mice because of the absence of the bisecting GlcNAc on their *N*-glycans. A mouse hepatocyte culture assay dependent on mouse serum for proliferation might provide evidence for this hypothesis and ultimately allow the identification of glycoproteins that require the bisecting GlcNAc to function.

ACKNOWLEDGMENTS

We thank Drs. Liang Zhu and Anthony N. Karnezis at Albert Einstein for helpful advice and discussions on PH.

REFERENCES

1. Bhaumik, M., Harris, T., Sundaram, S., Johnson, L., Guttenplan, J., Rogler, C., and Stanley, P. Progression of hepatic neoplasms is severely retarded in mice lacking the bisecting *N*-acetylglucosamine on *N*-glycans: evidence for a glycoprotein factor that facilitates hepatic tumor progression. Cancer Res., *58:* 2881–2887, 1998.
2. Yang, X., Bhaumik, M., Bhattacharyya, R., Gong, S., Rogler, C. E., and Stanley, P. New evidence for an extra-hepatic role of *N*-acetylglucosaminyltransferase III in the progression of diethylnitrosamine-induced liver tumors in mice. Cancer Res., *60:* 3313–3319, 2000.
3. Granovsky, M., Fata, J., Pawling, J., Muller, W. J., Khokha, R., and Dennis, J. W. Suppression of tumor growth and metastasis in Mgat5-deficient mice. Nat. Med., *6:* 306–312, 2000.
4. Leppanen, A., White, S. P., Helin, J., McEver, R. P., and Cummings, R. D. Binding of glycosulfopeptides to P-selectin requires stereospecific contributions of individual tyrosine sulfate and sugar residues. J. Biol. Chem., *275:* 39569–39578, 2000.
5. Kim, Y. J., Borsig, L., Varki, N. M., and Varki, A. P-Selectin deficiency attenuates tumor growth and metastasis. Proc. Natl. Acad. Sci. USA, *95:* 9325–9330, 1998.
6. Ohyama, C., Tsuboi, S., and Fukuda, M. Dual roles of sialyl Lewis X oligosaccharides in tumor metastasis and rejection by natural killer cells. EMBO J., *18:* 1516–1525, 1999.
7. Ohyama, C., Kanto, S., Kato, K., Nakano, O., Arai, Y., Kato, T., Chen, S., Fukuda, M. N., and Fukuda, M. Natural killer cells attack tumor cells expressing high levels of sialyl Lewis x oligosaccharides. Proc. Natl. Acad. Sci. USA, *99:* 13789–13794, 2002.
8. Hakomori, S. Glycosylation defining cancer malignancy: new wine in an old bottle. Proc. Natl. Acad. Sci. USA, *99:* 10231–10233, 2002.
9. Priatel, J. J., Sarkar, M., Schachter, H., and Marth, J. D. Isolation, characterization and inactivation of the mouse Mgat3 gene: the bisecting *N*-acetylglucosamine in asparagine-linked oligosaccharides appears dispensable for viability and reproduction. Glycobiology, *7:* 45–56, 1997.
10. Bhattacharyya, R., Bhaumik, M., Raju, T. S., and Stanley, P. Truncated, inactive *N*-acetylglucosaminyltransferase III (GlcNAc-TIII) induces neurological and other traits absent in mice that lack GlcNAc-TIII. J. Biol. Chem., *277:* 26300–26309, 2002.
11. Pospisil, J., Vlaskova, J., Pouckova, P., and Polivkova, J. The effect of phenobarbital on the development of tumors induced by methylcholanthrene in mice of various inbred strains. Sb. Lek., *88:* 131–138, 1986.
12. Yamaguchi, R., Yano, H., Iemura, A., Ogasawara, S., Haramaki, M., and Kojiro, M. Expression of vascular endothelial growth factor in human hepatocellular carcinoma. Hepatology, *28:* 68–77, 1998.
13. Claffey, K. P., Senger, D. R., and Spiegelman, B. M. Structural requirements for dimerization, glycosylation, secretion, and biological function of VPF/VEGF. Biochim. Biophys. Acta, *1246:* 1–9, 1995.
14. Peretz, D., Gitay-Goren, H., Safran, M., Kimmel, N., Gospodarowicz, D., and Neufeld, G. Glycosylation of vascular endothelial growth factor is not required for its mitogenic activity. Biochem. Biophys. Res. Commun., *182:* 1340–1347, 1992.
15. Kitada, T., Miyoshi, E., Noda, K., Higashiyama, S., Ihara, H., Matsuura, N., Hayashi, N., Kawata, S., Matsuzawa, Y., and Taniguchi, N. The addition of bisecting *N*-acetylglucosamine residues to E-cadherin down-regulates the tyrosine phosphorylation of β-catenin. J. Biol. Chem., *276:* 475–480, 2001.
16. Pascale, R., Narasimhan, S., and Rajalakshmi, S. Expression of *N*-acetylglucosaminyltransferase III in hepatic nodules generated by different models of rat liver carcinogenesis. Carcinogenesis (Lond.), *10:* 961–964, 1989.
17. Nishikawa, A., Gu, J., Fujii, S., and Taniguchi, N. Determination of *N*-acetylglucosaminyltransferases III, IV and V in normal and hepatoma tissues of rats. Biochim. Biophys. Acta, *1035:* 313–318, 1990.
18. Nishikawa, A., Fujii, S., Sugiyama, T., Hayashi, N., and Taniguchi, N. High expression of an *N*-acetylglucosaminyltransferase III in 3′-methyl DAB-induced hepatoma and ascites hepatoma. Biochem. Biophys. Res. Commun., *152:* 107–112, 1988.
19. Narasimhan, S., Schachter, H., and Rajalakshmi, S. Expression of *N*-acetylglucosaminyltransferase III in hepatic nodules during rat liver carcinogenesis promoted by orotic acid. J. Biol. Chem., *263:* 1273–1281, 1988.
20. Narasimhan, S., Lee, J. W., Cheung, R. K., Gelfand, E. W., and Schachter, H. β-1,4-Mannosyl-glycoprotein β-1,4-*N*-acetylglucosaminyltransferase III activity in human B and T lymphocyte lines and in tonsillar B and T lymphocytes. Biochem. Cell Biol., *66:* 889–900, 1988.
21. Ishibashi, K., Nishikawa, A., Hayashi, N., Kasahara, A., Sato, N., Fujii, S., Kamada, T., and Taniguchi, N. *N*-Acetylglucosaminyltransferase III in human serum, and liver and hepatoma tissues: increased activity in liver cirrhosis and hepatoma patients. Clin. Chim. Acta, *185:* 325–332, 1989.
22. Lee, G. H. Paradoxical effects of phenobarbital on mouse hepatocarcinogenesis. Toxicol. Pathol., *28:* 215–225, 2000.
23. Meyer, U. A., and Hoffmann, K. Phenobarbital-mediated changes in gene expression in the liver. Drug Metab. Rev., *31:* 365–373, 1999.
24. Miura, H., Miyazaki, T., Kuroda, M., Oka, T., Machinami, R., Kodama, T., Shibuya, M., Makuuchi, M., Yazaki, Y., and Ohnishi, S. Increased expression of vascular endothelial growth factor in human hepatocellular carcinoma. J. Hepatol., *27:* 854–861, 1997.
25. Shimizu, H., Miyazaki, M., Wakabayashi, Y., Mitsuhashi, N., Kato, A., Ito, H., Nakagawa, K., Yoshidome, H., Kataoka, M., and Nakajima, N. Vascular endothelial growth factor secreted by replicating hepatocytes induces sinusoidal endothelial cell proliferation during regeneration after partial hepatectomy in rats. J. Hepatol., *34:* 683–689, 2001.
26. Kang, R., Ikeda, Y., Miyoshi, E., Wang, W., Li, W., Ihara, Y., Sheng, Y., and Taniguchi, N. Cell cycle-dependent regulation of *N*-acetylglucosaminyltransferase-III in a human colon cancer cell line, Colo201. Arch. Biochem. Biophys., *374:* 52–58, 2000.
27. Guo, H. B., Jiang, A. L., Ju, T. Z., and Chen, H. L. Opposing changes in *N*-acetylglucosaminyltransferase-V and -III during the cell cycle and all-*trans*-retinoic acid treatment of hepatocarcinoma cell line. Biochim. Biophys. Acta, *1495:* 297–307, 2000.
28. Fausto, N. Liver regeneration. J. Hepatol., *32:* 19–31, 2000.
29. Rebbaa, A., Yamamoto, H., Saito, T., Meuillet, E., Kim, P., Kersey, D. S., Bremer, E. G., Taniguchi, N., and Moskal, J. R. Gene transfection-mediated overexpression of β1, 4-*N*-acetylglucosamine bisecting oligosaccharides in glioma cell line U373 MG inhibits epidermal growth factor receptor function. J. Biol. Chem., *272:* 9275–9279, 1997.
30. Sato, Y., Takahashi, M., Shibukawa, Y., Jain, S. K., Hamaoka, R., Miyagawa, J., Yaginuma, Y., Honke, K., Ishikawa, M., and Taniguchi, N. Overexpression of *N*-acetylglucosaminyltransferase III enhances the epidermal growth factor-induced phosphorylation of ERK in HeLaS3 cells by up-regulation of the internalization rate of the receptors. J. Biol. Chem., *276:* 11956–11962, 2001.
31. Chen, G., Guan, M., Su, B., and Lu, Y. mRNA expression of three glycosyltransferases in human hepatoma tissues. Clin. Chim. Acta, *313:* 77–80, 2001.
32. Song, E. Y., Kang, S. K., Lee, Y. C., Park, Y. G., Chung, T. H., Kwon, D. H., Byun, S. M., and Kim, C. H. Expression of bisecting *N*-acetylglucosaminyltransferase-III in human hepatocarcinoma tissues, fetal liver tissues, and hepatoma cell lines of Hep3B and HepG2. Cancer Investig., *19:* 799–807, 2001.
33. Miyoshi, E., Ihara, Y., Nishikawa, A., Saito, H., Uozumi, N., Hayashi, N., Fusamoto, H., Kamada, T., and Taniguchi, N. Gene expression of *N*-acetylglucosaminyltransferases III and V: a possible implication for liver regeneration. Hepatology, *22:* 1847–1855, 1995.